Mon. Not. R. Astron. Soc. **384,** 548–562 (2008) doi:10.1111/j.1365-2966.2007.12523.x

A simple analytical formulation for periodic orbits in binary stars

Erick Nagel[1⋆] and Barbara Pichardo[1,2]

[1]*Instituto de Astronomía, Universidad Nacional Autónoma de México, Apdo. Postal 70-264, 04510, México, D. F., México*
[2]*Institute for Theoretical Physics, University of Zurich, Winterthurerstrasse 190, Zurich 8057, Switzerland*

Accepted 2007 October 1. Received 2007 August 22; in original form 2007 May 25

ABSTRACT

An analytical approximation to periodic orbits in the circular restricted three-body problem is provided. The formulation given in this work is based on calculations known from classical mechanics, but with the addition of certain terms necessary to give a reasonably good approximation. The results are compared with simulations. The derived simple set of analytical expressions gives periodic orbits on the discs of binary systems without the need to solve the equations of motion by numerical integration.

Key words: circumstellar matter – binaries:general.

1 INTRODUCTION

The majority of low-mass main-sequence stars seem to be grouped in multiple systems, particularly binary ones (Duquennoy & Mayor 1991; Fischer & Marcy 1992). These systems have attracted more attention since the discovery, from observations of excess radiation at infrared to millimetre waves and direct radio images, that many T Tauri and other pre-main-sequence binary stars possess both circumstellar and circumbinary discs (Rodríguez et al. 1998; for a review see Mathieu 1994; Mathieu et al. 2000). Improvements in observational techniques allow theories on these objects to be tested. Moreover, extrasolar planets have been found to orbit stars with a stellar companion, for example 16 Cygni B, τ Bootis and 55 ρ Cancri (Butler et al. 1997; Cochran et al. 1997). All these factors, as well as the possibility of stable orbits that could be populated by gas or particles, make the study of stellar discs in binary systems a key element in understanding stellar and planetary formation.

In particular, the study of the simple periodic orbits of a test particle in the restricted three-body problem results in a very good approximation to the streamlines in an accretion disc in a very small pressure and viscosity regime, or to proto-planetary systems and their debris (Kuiper belt objects). Extensive theoretical work has been carried out in this direction (Lubow & Shu 1975; Paczyński 1977; Papaloizou & Pringle 1977; Rudak & Paczyński 1981; Bonnell & Bastien 1992; Bate 1997; Bate & Bonnell 1997).

Several studies have focused on finding the simplest and most important geometric characteristics of the discs, namely the size of both the circumstellar and circumbinary discs, using analytical approximations: Eggleton (1983) provided a simple analytical approximation to the Roche lobes; Holman & Wiegert (1999) to radii in planetary discs; and Pichardo, Sparke & Aguilar (2005, PSA05 hereafter) to radii in eccentric binary stars.

Based on the approximation of classical mechanics to periodic orbits given by Moulton (1963), we calculate here the terms necessary to give a fairly good approximation to periodic orbits for the case of circular binaries. This formulation gives not only the radii of the circumstellar and circumbinary discs, but also a good description, in the form of an analytical approximation, of any periodic orbit at a given radius for either of the discs. Thus, the set of equations we provide can be used to find any periodic orbit or its initial conditions to run it directly in simulations of the three-body restricted problem, or as a good approximation to initial conditions in the eccentric case as well, from the point of view of particle or hydrodynamical simulations, without the need to solve the restricted three-body problem numerically.

The low-viscosity regime described by the periodic orbit representation is important in astrophysics because it gives an idea of how bodies would respond if they were influenced only by the effects of the potential exerted by the binaries, and it could enable the periodic orbits to be linked to physical unknown characteristics of the discs, such as viscosity, which need to be artificially introduced to hydrodynamical codes. It also might permit the calculation of physical characteristics such as dissipation rates, etc. Studies like these are easily addressed using approximated analytical expressions, instead of the usual numerical approximations to the periodic orbits, as an analytical formulation is much faster to add to any hydrodynamical or particle code that requires the characteristics of a given family of periodic orbits, or simply their initial conditions in a more precise form than assuming Keplerian discs until the approximation fails. The periodic orbits show regions where the orbits are compressed (or decompressed); these regions could trigger density fluctuations that may be able to drive material to form

⋆E-mail: e.nagel@astrosmo.unam.mx

important agglomerations in the discs, which, depending on their positions in the disc and the density, could give rise to planets. An analytical approximation with a given density law for the discs would make these kinds of studies much faster and easier.

In Section 2, we give the strategy and equations used to find the approximation to periodic orbits in circumstellar discs. In Section 3, we present the equations approximating periodic orbits in circumbinary discs, and include an analysis of stability in Section 3.2. A comparison of the applications of this formulation and of numerically calculated periodic orbits is given in Section 4. Conclusions are presented in Section 5.

2 METHODOLOGY

In general, orbits around binary systems are calculated by approximate methods. Numerical calculations are the most common. In this work we use a perturbative analysis, an alternative method, to search for an analytical approximation that will provide solutions for any orbit in the circumbinary or circumstellar discs for the circular problem. The method is based on a perturbative analysis. Here, we choose the terms to be perturbed from the expanded equations of motion according to which were relevant to the solution of the problem. The original equations are approximated with a set of equations that, in many cases, have an analytical solution. Compared with the numerical approach, this approach has the advantage that the expressions are completely analytical and simple. We compare our calculations with numerical studies in order to pick as many terms in the expansion as we need to obtain the solution. The method can be used as a way to find a quick answer, and for studies in which an analytic expression makes the problem manageable.

2.1 Periodic orbits in circumstellar discs

The analysis is restricted to the orbital plane. In polar coordinates, the equations of motion are given by

$$\begin{aligned} \ddot{r} - r\dot{\psi}^2 &= F_r, \\ r\ddot{\psi} + 2\dot{r}\dot{\psi} &= F_\psi, \end{aligned} \tag{1}$$

where the origin of the system is located at the position of the star with mass M_1 (hereafter we call this star S_1). It is important to note that S_1 can represent either the primary or the secondary star. Here, r and ψ are the radial and angular coordinates, respectively, and the forces along the direction (F_r, F_ψ) have the form

$$\begin{aligned} F_r &= -\frac{GM_1}{r^2} + GM_2\frac{\partial\Phi_\mathrm{p}}{\partial r}, \\ F_\psi &= \frac{GM_2}{r}\frac{\partial\Phi_\mathrm{p}}{\partial\psi}, \end{aligned}$$

with

$$\Phi_\mathrm{p} = \frac{1}{(R^2 - 2rR\cos(\psi-\Psi) + r^2)^{1/2}} - \frac{r\cos(\psi-\Psi)}{R^2}, \tag{2}$$

which represents the perturbing potential (divided by GM_2) arising from the star with mass M_2 (hereafter, star S_2). Φ_p could be expressed in terms of the Legendre polynomials (Murray & Dermott 1999). Here, R and Ψ are the coordinates of S_2, and r and ψ locate the particle that is perturbed, P.

The non-perturbed state corresponds to the case with $\Phi_\mathrm{p} = 0$. Thus, the non-perturbed orbits are conics around S_1, and are perturbed by the presence of the other mass. The set of equations (1) cannot be solved analytically, so we expand the perturbation given in equation (2) using r/R as a small parameter. At some points in an orbit that begins around a resonance this parameter is large, so this approach is not valid. This expansion improves in precision the closer the particle is to S_1. Thus, equations (1) can be written as

$$\begin{aligned} \ddot{r} - r\dot{\psi}^2 + \frac{GM_1}{r^2} &= \frac{GM_2}{2}\frac{r}{R^3}\left[(1+3\cos 2(\psi-\Psi)) + \frac{3}{4}\frac{r}{R}(3\cos(\psi-\Psi) + 5\cos 3(\psi-\Psi))\right. \\ &\quad \left. + \left(\frac{r}{R}\right)^2\left(\frac{9}{8} + \frac{5}{2}\cos 2(\psi-\Psi) + \frac{35}{8}\cos 4(\psi-\Psi)\right) + ...\right], \\ r\ddot{\psi} + 2\dot{r}\dot{\psi} &= -\frac{GM_2}{2}\frac{r}{R^3}\left[(3\sin 2(\psi-\Psi)) + \frac{3}{4}\frac{r}{R}(\sin(\psi-\Psi) + 5\sin 3(\psi-\Psi))\right. \\ &\quad \left. + \frac{5}{4}\left(\frac{r}{R}\right)^2\left(\sin 2(\psi-\Psi) + \frac{7}{2}\sin 4(\psi-\Psi)\right) + ...\right], \end{aligned} \tag{3}$$

which is equivalent to the expansion (6.22) in Murray & Dermott (1999).

In this analysis, the star S_2 is in a circular orbit around S_1. We consider the mass of the discs to be negligible compared with the mass of the binary system. Thus, the orbit of S_2 is given by

$$\begin{aligned} R &= a, \\ \Psi &= \sqrt{\frac{G(M_1+M_2)}{a^3}}(t-t_0) = \Omega(t-t_0), \end{aligned} \tag{4}$$

where a represents the fixed distance between the stars, and Ω is the angular velocity of S_2 from Kepler's third law. At $t = t_0$ the star is in the reference line, which for a circular orbit can be any radial line that begins on S_1. The non-perturbed trajectory of the particle P is a Keplerian orbit around S_1, and the polar coordinates are expressed as

$$\begin{aligned} r &= a_{\rm np}, \\ \psi &= \sqrt{\frac{GM_1}{a_{\rm np}^3}}(t - t_0) = \omega(t - t_0), \end{aligned} \tag{5}$$

where $a_{\rm np}$ and ω have the same meaning as their counterparts in equation (4), but relating to P and S_1.

The perturbed position of the particle P can be written

$$r = a_{\rm np}(1 + r_{\rm p}), \tag{6}$$

$$\psi = \omega(t - t_0) + \psi_{\rm p}, \tag{7}$$

where the terms ($a_{\rm np}\ r_{\rm p}$) and $\psi_{\rm p}$ are the corrections in the trajectory resulting from the presence of S_2. We now define the parameters $m_{\rm o}$ and τ as follows:

$$m_{\rm o} = \frac{\Omega}{\omega - \Omega}, \tag{8}$$

$$\tau = (\omega - \Omega)(t - t_0), \tag{9}$$

where $m_{\rm o}$ is a small parameter for $r \ll R$. This condition is required for the expansion of the equations of motion (equations 3) to be useful. τ is the angle that locates the particle P, measured from the line connecting the stars, for the non-perturbed orbit. The first step is to replace t by τ in equation (3), using equation (9). Equations (6) and (7) are substituted in equations (3), taking into account that $r_{\rm p}$ and $\psi_{\rm p}$ depend on τ. The resulting expressions are finally divided by $a_{\rm np}(\Omega/m_{\rm o})^2$. The mass is given in units of $M_1 + M_2$, and $M_1 + M_2 = 1$. Thus,

$$\begin{aligned} &\ddot{r_{\rm p}} - (1 + r_{\rm p})(1 + m_{\rm o} + \dot{\psi}_{\rm p})^2 + \frac{(1 + m_{\rm o})^2}{(1 + r_{\rm p})^2} \\ &= \frac{m_{\rm o}^2 M_2}{2}(1 + r_{\rm p})[(1 + 3\cos 2(\tau + \psi_{\rm p})) \\ &\quad + \frac{3}{4}{\rm H}m_{\rm o}(1 + r_{\rm p})(3\cos(\tau + \psi_{\rm p}) + 5\cos 3(\tau + \psi_{\rm p})) \\ &\quad + {\rm H}^2 m_{\rm o}^2(1 + r_{\rm p})^2(\frac{9}{8} + \frac{5}{2}\cos 2(\tau + \psi_{\rm p}) + \frac{35}{8}\cos 4(\tau + \psi_{\rm p})) \\ &\quad + ...], \end{aligned} \tag{10}$$

$$\begin{aligned} &(1 + r_{\rm p})\ddot{\psi}_{\rm p} + 2\dot{r_{\rm p}}(1 + m_{\rm o} + \dot{\psi}_{\rm p}) \\ &= -\frac{m_{\rm o}^2 M_2}{2}(1 + r_{\rm p})[3\sin 2(\tau + \psi_{\rm p}) \\ &\quad + \frac{3}{4}{\rm H}m_{\rm o}(1 + r_{\rm p})(\sin(\tau + \psi_{\rm p}) + 5\sin 3(\tau + \psi_{\rm p})) \\ &\quad + \frac{5}{4}{\rm H}^2 m_{\rm o}^2(1 + r_{\rm p})^2(\sin 2(\tau + \psi_{\rm p}) + \frac{7}{2}\sin 4(\tau + \psi_{\rm p})) \\ &\quad + ...]. \end{aligned} \tag{11}$$

Equations (10) and (11) are dimensionless. They will be solved for $r_{\rm p}$ and $\psi_{\rm p}$ in terms of M_2 ($M_1 = 1 - M_2$), τ and $m_{\rm o}$. The value for M_2 characterizes the stellar masses of the system, τ defines the angular position of the point on the original non-perturbed orbit, and $m_{\rm o}$ depends on the radial position of the non-perturbed trajectory $a_{\rm np}$, in units of the separation between the stars, a. An analytic solution is found if an expansion for $r_{\rm p}$ and $\psi_{\rm p}$ in powers of $m_{\rm o}$ is made as follows:

$$r_{\rm p} = \Sigma_{j=2}^{\infty} r_{{\rm p}_j}(M_2, \tau) m_{\rm o}^j, \tag{12}$$

$$\psi_{\rm p} = \Sigma_{j=2}^{\infty} \psi_{{\rm p}_j}(M_2, \tau) m_{\rm o}^j. \tag{13}$$

Specifically, for periodic orbits, it is necessary to fulfil the following conditions:

$$\begin{aligned} r_{p_j}(\tau + 2\pi) &= r_{{\rm p}_j}(\tau), \\ \psi_{p_j}(\tau + 2\pi) &= \psi_{{\rm p}_j}(\tau). \end{aligned} \tag{14}$$

A useful assumption is that the angular position of the orbit, from the line that connects the two stars, is not perturbed by S_2, which can be proved by symmetry. We restrict the perturbed orbits to be symmetric with respect to the line joining the stars by

$$\psi_{\mathrm{p}_j}(0) = 0. \tag{15}$$

This condition is general enough, as there are no restrictions from observations concerning the orientation of the symmetry axis in the plane of the discs with respect to the line joining the stars.

Equations (12) and (13) are substituted in equations (10) and (11) and expanded in powers of m_{o}, resulting in a polynomial in m_{o} equal to zero. The only solution for such an equation is that every coefficient is zero. Each coefficient associated with a given power is a second-order differential equation. The solutions of the equations for $m^k{}_{\mathrm{o}}$ with $k = 2, 3, 4$ are solved by imposing the conditions given in equations (14) and (15), and are given by

$$r_{\mathrm{p}_2} = -\frac{M_2}{6} + \frac{15}{16} H M_2 \cos\tau - M_2 \cos 2\tau, \tag{16}$$

$$\psi_{\mathrm{p}_2} = -\frac{15}{8} H M_2 \sin\tau + \frac{11 M_2}{8} \sin 2\tau, \tag{17}$$

$$r_{\mathrm{p}_3} = \frac{M_2}{3} + \left(\frac{135}{32} H M_2^2 - \frac{3}{32} H M_2\right) \cos\tau - \frac{7}{6} M_2 \cos 2\tau - \frac{25}{64} H M_2 \cos 3\tau, \tag{18}$$

$$\psi_{\mathrm{p}_3} = -\left(\frac{135}{16} H M_2^2 + \frac{21}{16} H M_2\right) \sin\tau + \frac{13}{6} M_2 \sin 2\tau + \frac{15}{32} H M_2 \sin 3\tau, \tag{19}$$

$$\begin{aligned} r_{\mathrm{p}_4} = {} & \frac{331}{288} M_2^2 - \frac{1}{2} M_2 + \frac{225}{512} H^2 M_2^2 - \frac{3}{16} H^2 M_2 + q_4 \cos\tau + \\ & \left(\frac{2}{3} M_2^2 - \frac{10}{9} M_2 - \frac{225}{512} H^2 M_2^2 - \frac{5}{8} H^2 M_2\right) \cos 2\tau + \\ & \left(\frac{255}{256} H M_2^2 - \frac{65}{256} H M_2\right) \cos 3\tau - \left(\frac{3}{8} M_2^2 + \frac{7}{32} H^2 M_2\right) \cos 4\tau, \end{aligned} \tag{20}$$

$$\begin{aligned} \psi_{\mathrm{p}_4} = {} & -\left(2q_4 + \frac{515}{64} H M_2^2 - \frac{3}{16} H M_2\right) \sin\tau + \left(-\frac{1}{2} M_2^2 + \frac{41}{18} M_2 + \frac{1125}{1024} H^2 M_2^2 + \frac{25}{32} H^2 M_2\right) \sin 2\tau \\ & + \left(-\frac{255}{128} H M_2^2 + \frac{55}{128} H M_2\right) \sin 3\tau + \left(\frac{201}{256} M_2^2 + \frac{63}{256} H^2 M_2\right) \sin 4\tau, \end{aligned} \tag{21}$$

with

$$q_4 = \frac{3}{64} M_2 H - \frac{1727}{256} M_2^2 H + \frac{1215}{64} M_2^3 H + \frac{105}{128} M_2 H^3. \tag{22}$$

It is worth noting that, for each order (in $m^k{}_{\mathrm{o}}$), we obtain a system of two differential equations that produces two integration constants that can be calculated by solving the set of equations of the next higher order, by imposing the conditions in equations (14) and (15).

The parameter H comes from the approximation $a_{\mathrm{np}} = m_{\mathrm{o}}\, H$, where we will consider H constant, justified by the fact that H depends weakly on m_{o} (Moulton 1963).

The use of equations (16) to (21), plus equations (12) and (13), in equations (6) and (7) will enable us to find the perturbed trajectory of the particle P. Because a_{np} is proportional to m_{o}, the radial corrections are of order m_{o}^5 and the angular corrections are of order m_{o}^4. Thus, equations (6) and (7) represent coordinates depending on time, which means that velocity and accelerations can be obtained by direct differentiation. It is worth noting that the orbits are given in a reference system in which the stars are fixed on the X-axis. Some examples of the orbits and rotation curves produced by this model are given in Section 4.

2.2 The radial extension of circumstellar discs

In order to calculate the total radial size of discs we will assume that we are in the regime of low-pressure gas. The gas can settle in permitted orbits which do not intersect themselves or any other (Paczyński 1977, PSA05). In this paper the disc radii is given by intersections of orbits, except that the intersections are found analytically (another analytical approximation to the radial extension for circumstellar discs for any eccentricity can be found in PSA05). First, we choose a given M_2 to fix the binary system. A physical intersection occurs when

$$r_2 - r_1 = 0, \tag{23}$$

$$\psi_2 - \psi_1 = 0, \tag{24}$$

where r_i is the radius of the orbit given by equation (6) and ψ_i spans the 2π angular range of the same orbit. The subindex i takes the values $i = 1, 2$ for inner and outer consecutive orbits, respectively. We now look for values for a_{np} and τ that simultaneously satisfy equations (23)

Table 1. Sizes of the circumstellar discs for various values of M_1.

M_1	$a_{\mathrm{np},\tau=\pi}$	$r(\tau=0)$	$r(\tau=\pi)$	$\langle r\rangle$	$\langle r\rangle_{\mathrm{PSA}}$	R_{RL}
0.1	0.1628	0.1641	0.1326	0.1484	0.125	0.213
0.2	0.2077	0.2113	0.1690	0.1901	0.162	0.268
0.3	0.2445	0.2486	0.1989	0.2237	0.195	0.308
0.4	0.2795	0.2825	0.2276	0.2550	0.228	0.344
0.5	0.3155	0.3155	0.2573	0.2864	0.257	0.379
0.6	0.3543	0.3489	0.2901	0.3195	0.317	0.414
0.7	0.3982	0.3841	0.3285	0.3563	0.350	0.454
0.8	0.4507	0.4236	0.3766	0.4001	0.387	0.501
0.9	0.5213	0.4774	0.4466	0.4620	0.426	0.570

Notes. Column 1 gives various values of M_1. Column 2 gives the solution of equation (25) for various values of M_1, with $\tau=\pi$. Columns 3 and 4 give the radial positions of the innermost intersecting orbit. The average of these values is given in Column 5. Column 6 gives the same average but from PSA05. Column 7 gives the approximation to the Roche lobe radius according to Eggleton (1983) given by equations (27), (28) and (29).

and (24). Note that equation (23) can be expanded in a Taylor series in the variable a_{np}. Because of the assumption that we are interested in infinitesimally close orbits, a linear approximation is good enough. Thus, equation (23) can be transformed to

$$\frac{\mathrm{d}r}{\mathrm{d}a_{\mathrm{np}}}=0, \tag{25}$$

which is a function of M_2, a_{np} and τ. Furthermore, using equation (7), equation (24) can be written as

$$\psi_{\mathrm{p},2}-\psi_{\mathrm{p},1}=0. \tag{26}$$

From equations (17), (19) and (21) we can directly identify that all the terms are proportional to $\sin(k\tau)$, which in turn means that equations (17), (19) and (21) are proportional to $\sin\tau$. Thus, $\sin\tau$ can be factorized in equation (26), giving the solutions $\tau=0$ and $\tau=\pi$. Equation (26) has other solutions, but none allows us to find a root for equation (25). Using either $\tau=0$ or $\tau=\pi$ in equation (25), we end up with an equation for a_{np}. The solution of equation (25) using $\tau=0$, π gives two values of a_{np}, which correspond to the intersections. We take the intersection at the smallest radius (which represents the maximum radii at which gas particles are able to follow the orbits), and thus the second intersection at the larger radius is not useful in this analysis. In both cases the intersecting orbits are tangent to each other, and contiguous orbits between them intersect at an angle. Because we do not consider these kinds of orbits to be part of the disc, the disc naturally ends up in the orbits with smaller a_{np}.

The minimum value for a_{np} comes from $\tau=\pi$; that is, the intersection appears at the side of S_2 opposite to S_1. In Table 1, the solution of equation (25) for various values of M_1, with $\tau=\pi$, is given in the column headed $a_{\mathrm{np},\tau=\pi}$. The following two columns ($r(\tau=0)$, $r(\tau=\pi)$) give the radial positions of the innermost intersecting orbit. The average of these values is given in the column $\langle r\rangle$; the next column gives the same average but from PSA05; and the final column is the approximation to the Roche lobe radius according to Eggleton (1983) given by

$$\frac{R_i}{a}\approx\frac{R_{i(\mathrm{Egg})}}{a}=\frac{0.49q_i^{2/3}}{0.6q_i^{2/3}+\ln(1+q_i^{1/3})}, \tag{27}$$

where

$$q_1=\frac{1-M_2}{M_2}, \tag{28}$$

$$q_2=\frac{M_2}{1-M_2}, \tag{29}$$

where i refers to star S_i with $i=1$ or 2.

From Table 1, $\langle r\rangle$ is at most 20 per cent away from $\langle r\rangle_{\mathrm{PSA}}$ (for particular masses of the stars, M_1 and $M_2=1-M_1$) for $M_1\leqslant 0.5$, decreasing to less than 10 per cent for $M_1>0.5$. As expected, the last non-intersecting orbit is contained inside the Roche lobe, as we can see in Fig. 1, for $M_2=0.2$. A good approximation for the Roche lobe is given using the approximation of Eggleton (1983).

3 ORBITS IN CIRCUMBINARY DISCS

The method described in Section 2.1 is followed here for orbits in circumbinary discs, with a few changes. First, the origin is now at the centre of mass of the system. The perturbing potential, Φ_{p}, takes the form

$$\Phi_{\mathrm{p}}=\frac{GM_1}{r}\left[1-\frac{2R_1}{r}\cos(\psi-\psi_1)+\left(\frac{R_1}{r}\right)^2\right]^{-1/2}+\frac{GM_2}{r}\left[1+\frac{2R_2}{r}\cos(\psi-\psi_1)+\left(\frac{R_2}{r}\right)^2\right]^{-1/2}, \tag{30}$$

where $R_1=M_2\,R$, $R_2=M_1\,R$ are the distances to the stars S_1 and S_2 from the origin, respectively. It is important to note that S_2 is located to the left of the centre of mass, and that it can represent either the secondary or the primary star. a is the distance between the stars. r and

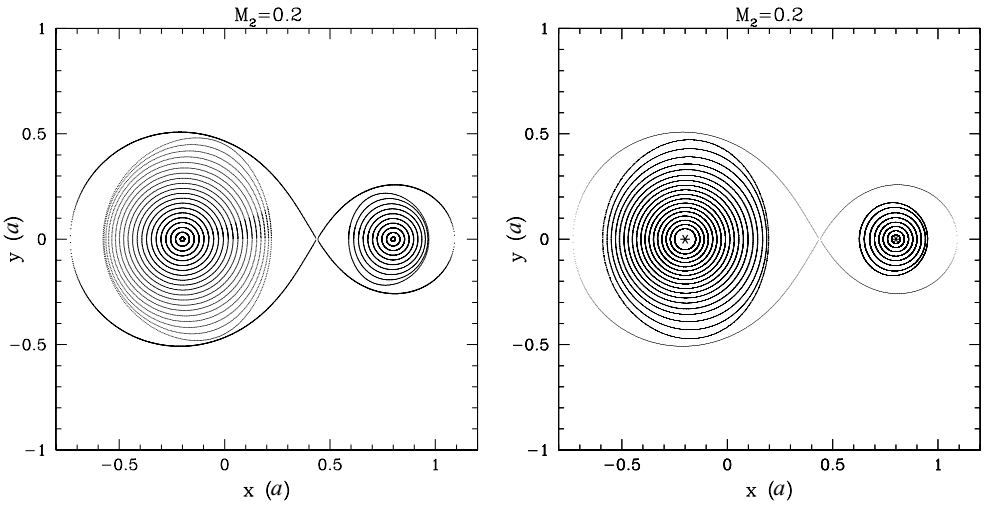

Figure 1. Comparison for a circumstellar disc between orbits obtained with the approximation presented in this work and with the numerical results described in Subsection 4.1 for the case $M_2 = 0.2$. The left panel shows the analytical approximation provided in this work, and the right panel shows the numerical approximation. The darker curve surrounding the discs is the Roche lobe. The axes are in units of the distance between the stars, a

$\psi - \psi_1$ are the coordinates for a particle P tracing a circumbinary orbit, where the angle is measured from the radial vector directed towards S_1. In this case, equation (1) can be used with the new definitions as follows:

$$F_r = \frac{\partial \Phi_{\rm p}}{\partial r}, \tag{31}$$

$$F_\psi = \frac{1}{r}\frac{\partial \Phi_{\rm p}}{\partial \psi}. \tag{32}$$

Thus, an expansion of equation (1) for $R_1/r \ll 1$ and $R_2/r \ll 1$ can be developed:

$$\begin{aligned} \ddot{r} - r\dot{\psi}^2 + \frac{G(M_1+M_2)}{r^2} &= -GM_{\rm p}\frac{a^2}{r^4}\left\{\frac{3}{4}[1+3\cos 2(\psi-\psi_1)]+\right. \\ &\left.\frac{R_1-R_2}{2r}[3\cos(\psi-\psi_1)+5\cos 3(\psi-\psi_1)]+\ldots\right\}, \\ r\ddot{\psi} + 2\dot{r}\dot{\psi} &= -GM_{\rm p}\frac{a^2}{r^4}\left\{\frac{3}{2}\sin 2(\psi-\psi_1)+\right. \\ &\left.\frac{3(R_1-R_2)}{8r}[\sin(\psi-\psi_1)+5\sin 3(\psi-\psi_1)]+\ldots\right\}, \end{aligned} \tag{33}$$

where $M_{\rm p} = M_1\, M_2 = M_2(1 - M_2)$.

The third term on the left-hand side of the first equation represents the contribution to the force when all the stellar mass is concentrated at the origin. The right-hand side of both equations is the perturbing force arising from the mass distribution between the stellar components. If the right-hand side of equation (33) is equal to zero, we find the non-perturbed orbit in the form

$$r = a_{\rm np}, \tag{34}$$

$$\psi = \sqrt{\frac{G(M_1+M_2)}{a_{\rm np}^3}}(t-t_0) = \omega(t-t_0). \tag{35}$$

Note that the definition of ω differs from that for the circumstellar case in terms of the mathematical expression; however, the meaning is the same, namely the non-perturbed angular velocity of the particle P. Again, the perturbed position of P is given by equations (6) and (7). Equation (9) changes to

$$\tau = (\Omega - \omega)(t - t_0), \tag{36}$$

where $\Omega = \sqrt{G(M_1+M_2)/a^3}$ is the angular velocity of the binary system, and τ represents the angle between S_1 and P.

A useful parameter is given by

$$\mu = \frac{\omega}{\Omega} = \left(\frac{a}{a_{\rm np}}\right)^{3/2}, \tag{37}$$

where μ is the parameter used to expand equation (33), and we note that μ is small as we are only taking into account circumbinary orbits far away from the stars. Changing $t \to \tau$ (equation 36) and expanding equation (33) in a power series of $\mu^{1/3}$, we can write the equations of

motion as

$$\ddot{r_{\rm p}} - (1+r_{\rm p})\left(\frac{\mu}{1-\mu}+\dot{\psi_{\rm p}}\right)^2 + \frac{\mu^2}{(1-\mu)^2}\frac{1}{(1+r_{\rm p})^2} = \\ -\frac{M_{\rm p}}{(1-\mu)^2}\frac{\mu^{10/3}}{(1+r_{\rm p})^4}\left\{\frac{3}{4}[1+3\cos 2(\tau+\psi_{\rm p})] \right. \\ \left. + \frac{(2M_2-1)\mu^{2/3}}{2(1+r_{\rm p})}[3\cos(\tau+\psi_{\rm p})+5\cos 3(\tau+\psi_{\rm p})]+...\right\}, \tag{38}$$

$$(1+r_{\rm p})\ddot{\psi_{\rm p}} + 2\dot{r_{\rm p}}\left(\frac{\mu}{1-\mu}+\dot{\psi_{\rm p}}\right) = \\ -\frac{M_{\rm p}}{(1-\mu)^2}\frac{\mu^{10/3}}{(1+r_{\rm p})^4}\left\{\frac{3}{2}\sin 2(\tau+\psi_{\rm p}) \right. \\ \left. + \frac{3}{8}\frac{(2M_2-1)\mu^{2/3}}{(1+r_{\rm p})}[\sin(\tau+\psi_{\rm p})+5\sin 3(\tau+\psi_{\rm p})]+...\right\}. \tag{39}$$

In the same way as in Section 2.1, differential equations are extracted at different orders if we expand $r_{\rm p}$ and $\psi_{\rm p}$ as follows:

$$r_{\rm p} = \Sigma_{i=4}^{\infty} r_{{\rm p}_i}(M_2,\tau)\mu^{i/3}, \tag{40}$$

$$\psi_{\rm p} = \Sigma_{i=4}^{\infty} \psi_{{\rm p}_i}(M_2,\tau)\mu^{i/3}. \tag{41}$$

The perturbed trajectories must be closed, which means that equation (14) must be satisfied. Moreover, the fact that the orbit is symmetric with respect to the line joining the two stars allows us to derive the condition

$$\dot{r_{{\rm p}_i}}(\tau=0) = 0. \tag{42}$$

Substitution of equations (40) and (41) into equations (38) and (39) gives two polynomials in $\mu^{i/3}$. A solution can be found if every coefficient of the $\mu^{i/3}$ terms is zero. Using the conditions given in equations (42) and (14) allows us to find the set of solutions.

Moulton (1963) describes the method and gives explicit expressions for r_{p_i} and ψ_{p_i} for $i \leqslant 15$. The integration constants with the full expressions are provided in the following equations:

$$\begin{aligned}
r_{\rm p4} &= \frac{1}{4}M_{\rm p}, \\
r_{\rm p5} &= 0, \\
r_{\rm p6} &= 0, \\
r_{\rm p7} &= 0, \\
r_{\rm p8} &= \frac{3}{64}M_{\rm p}\left(5(1-M_2)^2 - 9M_{\rm p} + 5M_2^2\right), \\
r_{\rm p9} &= 0, \\
r_{\rm p10} &= \frac{9}{16}M_{\rm p}^2\cos 2\tau, \\
r_{\rm p11} &= 0, \\
r_{\rm p12} &= \frac{1}{768}M_{\rm p}\left(175(1-M_2)^4 - 535(1-M_2)^3M_2 + 711(1-M_2)^2M_2^2 - 535(1-M_2)M_2^3 + 175M_2^4\right) \\
&\quad -\frac{M_{\rm p}}{2}(1-2M_2)\left(3\cos\tau + \frac{5}{9}\cos 3\tau\right), \\
r_{\rm p13} &= \frac{3}{4}M_{\rm p}\cos 2\tau, \\
r_{\rm p14} &= -\frac{39}{32}M_{\rm p}^2 + \frac{M_{\rm p}}{64}\left(25(1-M_2)^2 - 61M_{\rm p} + 25M_2^2\right)\cos 2\tau + \\
&\quad \frac{175}{1024}M_{\rm p}\left((1-M_2)^2 - M_{\rm p} + M_2^2\right)\cos 4\tau, \\
r_{\rm p15} &= -\frac{9}{4}M_{\rm p}(1-2M_2)\left(\cos\tau + \frac{5}{27}\cos 3\tau\right),
\end{aligned} \tag{43}$$

Table 2. Size of the central gap in the circumbinary disc for various values of M_1.

M_1	$a_{\mathrm{np},\tau=0}$	$r(\tau=0)$	$r(\tau=\pi)$	$r(\tau=0)_{\mathrm{PSA}}$	$r(\tau=\pi)_{\mathrm{PSA}}$
0.1	1.3547	1.5660	1.2956	1.87	1.80
0.2	1.3920	1.6267	1.3509	2.04	2.00
0.3	1.3733	1.6179	1.3637	1.94	1.90
0.4	1.3131	1.5604	1.3642	1.92	1.90
0.5	1.1643	1.4183	1.4183	2.00	2.00

Notes. Column 1 gives various values of M_1. Column 2 give the non-perturbed radius a_{np}. Columns 3 and 4 give the physical radius of the orbit at the intersection with the line connecting the stars [$r(\tau=0)$ and $r(\tau=\pi)$, respectively]. Columns 5 and 6 give the analogous values in PSA05.

and for the angle we have

$$
\begin{aligned}
\psi_{\mathrm{p}4} &= 0,\\
\psi_{\mathrm{p}5} &= 0,\\
\psi_{\mathrm{p}6} &= 0,\\
\psi_{\mathrm{p}7} &= 0,\\
\psi_{\mathrm{p}8} &= 0,\\
\psi_{\mathrm{p}9} &= 0,\\
\psi_{\mathrm{p}10} &= \frac{3}{8}M_{\mathrm{p}}\sin 2\tau,\\
\psi_{\mathrm{p}11} &= 0,\\
\psi_{\mathrm{p}12} &= -\frac{3}{8}M_{\mathrm{p}}(1-2M_2)\left(\sin\tau+\frac{5}{9}\sin 3\tau\right),\\
\psi_{\mathrm{p}13} &= \frac{3}{16}M_{\mathrm{p}}\sin 2\tau,\\
\psi_{\mathrm{p}14} &= \frac{5}{32}M_{\mathrm{p}}\left((1-M_2)^2-4M_{\mathrm{p}}+M_2^2\right)\sin 2\tau+\frac{35}{256}M_{\mathrm{p}}\left((1-M_2)^2-M_{\mathrm{p}}+M_2^2\right)\sin 4\tau,\\
\psi_{\mathrm{p}15} &= \frac{1}{4}M_{\mathrm{p}}(1-2M_2)\left(9\sin\tau-\frac{25}{27}\sin 3\tau\right),
\end{aligned}
\tag{44}
$$

where the integration constant for the radial equation (38) is calculated using the solution for six orders ahead, whereas for the angular equation (39) the integration constant is obtained from the solution for 10 orders ahead.

It is worth noting that the approximation to circumbinary periodic orbits given by Moulton is far from the solution as we have compared with the numerical solution, thus we have developed all the necessary terms in the expansion of the potential to reach a fairly good approximation to the numerical solution of the problem.

In this way, an analytical expression is found for circumbinary orbits with high accuracy using expressions (43) and (44), and equations (40), (41), (37), (6) and (7).

3.1 The radial extension of circumbinary discs (the *Gap*)

Our purpose in this section is to provide a good estimate for the radius of the inner boundary of a circumbinary disc. We are thus looking for the stable orbit closest to the binary system. In this case, it is necessary to calculate orbits decreasing in size until consecutive orbits intersect each other. The procedure we followed was to find a few new terms in the approximate solution for the disturbed orbit and calculate the larger inner orbit that intersects a contiguous one using the method described in Section 2.2. In this case, as in the circumstellar disc calculation (see Section 2.2), the angular correction ψ_{p_i} is proportional to $\sin\tau$, and the intersections occur in the same manner at $\tau=0$ and $\tau=\pi$, i.e. on the line joining the stars. The larger the number of terms considered for the approximation, the closer the orbit is to the orbit calculated in PSA05. However, the difference in sizes is large, in spite of taking into account the terms up to $\mu^{21/3}=(a_{\mathrm{np}}/a)^{-21/2}$, which gives a high precision in the circumstellar disc case. Table 2 gives, for a set of values for M_1, the non-perturbed radius a_{np}, the physical radius of the orbit at the intersection with the line connecting the stars, $r(\tau=0)$ and $r(\tau=\pi)$, and the analogous values in PSA05. Here, for each M_1 there is an intersection at $\tau=0$ or at $\tau=\pi$. Note that, for example, the system with $M_1=0.2$ is the same system as the one with $M_1=0.8$, only rotated by an angle π; thus, the intersection at $a_{\mathrm{np}}=1.3920$ with $\tau=0$ in the former case corresponds to $a_{\mathrm{np}}=1.3920$ with $\tau=\pi$ in the latter. Thus, Table 2 gives radii for $M_1\leqslant 0.5$.

3.2 Stability analysis

In the numerical approach, the solution for a closed orbit is searched for by successive iterations. This means that an unstable orbit (surrounded by orbits far from the solution) is very hard to find. Unlike the case for numerical calculations, analytically one can calculate either stable or unstable orbits without any way to identify between them. One has to apply another criterion to look for the long-lived orbits such as the ones in real discs; this criterion is taken from a stability analysis.

In the case of circumstellar discs, the criterion to find the edge of the disc was the intersection of orbits. In the case of circumbinary discs, this is not applicable, because in general orbits start to be unstable before any intersection of orbits.

Message (1959) defines an orbit as stable or unstable using the equation that describes normal displacements from a periodic orbit in the three-body restricted problem. These displacements are solved with terms proportional to exp (i $c\tau$), where c is given by

$$c^4 - (4 + \lambda_{-1} + \lambda_1)c^2 + 2(\lambda_1 - \lambda_{-1})c + \lambda_{-1}\lambda_1 - \nu_1\nu_{-1} = 0, \tag{45}$$

where

$$\lambda_{\pm1} = \theta_0 - 1 - (\beta_0 + \beta_{\pm2})\theta_1\theta_{-1} - \beta_{\pm2}^2\beta_{\pm3}\theta_1^2\theta_{-1}^2, \tag{46}$$

$$\nu_{\pm1} = -\beta_0\theta_{\pm1}^2, \tag{47}$$

$$\beta_k = \frac{1}{\theta_0 - (k + c)^2}, \tag{48}$$

and θ_0, $\theta_{\pm1}$ are the main coefficients in the Fourier expansion of $\Theta(\tau)$, where $\Theta(\tau)$ is the function involved in the normal equation displacement,

$$\frac{\mathrm{d}^2q}{\mathrm{d}\tau^2} + \Theta(\tau)q = 0, \tag{49}$$

which is given in Message (1959). The function $\Theta(\tau)$ depends on the shape of the orbit, i.e. on τ. If, for a specific orbit, c has an imaginary part, the orbit is unstable. Calculation of c is made for analytical orbits given by equations (6) and (7) with r_p and ψ_p estimated with equations (40) and (41) and the coefficients given by equations (43) and (42). Orbits smaller and larger than the intersecting orbits given in Table 2 are considered. The values taken for the parameter a_np are given in Table 3.

The orbit found in PSA05 corresponds to an analytical orbit with the parameter $a = a_{np,\mathrm{PSA}}$. Thus, if this set of orbits is (un)stable we expect that the numerical orbits are also (un)stable. We solve equation (45) for the orbits in Table 3, and the results are given in Table 4. It can be seen that the largest values of the imaginary part of c, looking at all the modes found, are given by M_1 in the range from 0.1 to 0.5.

From Table 4, the trend for $Max|Im(c)|$ is to decrease when the orbit is moving away from the binary system, as expected. Note that $Max|Im(c(a_{np,\mathrm{PSA}}))|$ is quite small; consequently, this value can be taken as a threshold for instability, and the orbit in PSA05 will naturally define the boundary between the unstable (not possible for gas orbits) and the stable (possible) part of the disc.

It is worth noting that this analysis can be applied to either numerical or analytical orbits. All the Fourier coefficients required are for functions that depend on the orbit. Thus, the stability analysis described here is general, and can be used with any orbit of the restricted circular three-body problem.

4 TEST: COMPARISON WITH NUMERICAL RESULTS

In this section we present a simple comparison between the results presented in this work and precise numerical results obtained with the usual methods to integrate the equations of motion in a circular binary potential. To do this we take two approaches: first, we provide a direct

Table 3. Values of the parameter a_np for the orbits studied in the instability analysis.

M_1	$a_{\mathrm{np},1}$	$a_{\mathrm{np,Inters}}$	$a_{\mathrm{np},2}$	$a_{\mathrm{np},3}$	$a_{\mathrm{np,PSA}}$	$a_{\mathrm{np},4}$
0.1	1.25	1.3547	1.45	1.65	1.80	2.75
0.2	1.29	1.3920	1.49	1.69	1.99	2.79
0.3	1.27	1.3733	1.47	1.67	1.87	2.77
0.4	1.21	1.3131	1.41	1.61	1.86	2.71
0.5	1.06	1.1643	1.26	1.46	1.96	2.56

Table 4. Maximum imaginary part of c for the orbits studied in the instability analysis.

$Max\|Im(c)\| \setminus M_1$	0.1	0.2	0.3	0.4	0.5
$c(a_{\mathrm{np},1})$	2.65×10^{-3}	5.64×10^{-3}	8.26×10^{-3}	9.38×10^{-3}	3.60×10^{-11}
$c(a_{\mathrm{np,Inters}})$	6.47×10^{-4}	1.43×10^{-3}	1.84×10^{-3}	1.62×10^{-3}	2.76×10^{-12}
$c(a_{\mathrm{np},2})$	2.35×10^{-4}	4.87×10^{-4}	5.83×10^{-4}	4.29×10^{-4}	4.35×10^{-13}
$c(a_{\mathrm{np},3})$	4.96×10^{-5}	9.24×10^{-5}	9.60×10^{-5}	5.53×10^{-5}	2.68×10^{-14}
$c(a_{\mathrm{np,PSA}})$	2.09×10^{-5}	2.07×10^{-5}	2.72×10^{-5}	9.87×10^{-6}	0
$c(a_{\mathrm{np},4})$	0	0	0	0	0

qualitative comparison between the numerical and the analytical approximations to some representative discs; and second, using a comparison between numerical and analytical approximations that includes velocities, are the corresponding rotation curves.

4.1 The numerical method

The equations of motion of a test particle are solved for the circular restricted three-body problem using an Adams integrator (from the NAG FORTRAN library). Cartesian coordinates are employed, with the origin at the centre of mass of the binary, in an inertial frame of reference. Here we look for the families of circumstellar and circumbinary orbits at a given stellar phase of the stars (equivalent to looking for the families in the non-inertial frame of reference). We calculate the Jacobi energy of test particles, in the non-inertial frame of reference comoving with the stars, as a diagnostic for the quality of the numerical integration, conserved within one part in 10^9 per binary period.

4.2 Geometrical comparison of discs

In the case of binary systems, it is well known that the shape and extension of discs are different from those associated with single stars, where the periodic orbits are circles with an unlimited (by the potential of the single star) radius. In binary systems, the stellar companion exerts forces able to open gaps, limiting the extension of the discs and producing at the same time deformations in the shape of the discs, making them visually different from those associated with single stars. In this section we compare the discs obtained with the analytical approximation provided in this work, with the numerical solution, and with the Keplerian approximation.

To construct the analytical circumstellar discs we have employed equations (6) and (7), which can be written in the inertial reference system as

$$r = a_{\rm np}(1 + r_{\rm p}), \tag{50}$$

$$\psi = \tau + \psi_{\rm p}, \tag{51}$$

with τ in the interval $[0, 2\pi]$.

In Fig. 1, we compare the periodic orbits for a circumstellar disc in a binary system obtained by the approximation presented in this work (left panel) and numerical calculations (right panel). The value for M_2 is indicated at the top of the figure. The darker curve represents the Roche lobe.

Likewise, in Fig. 2 we show a qualitative comparison of a circumbinary disc for the analytical approximation (left panel) and numerical calculations (right panel). The distances of the stars with respect the centre of mass of the binary are shown.

The discs present a slight deformation of the orbits, depending on the radius: the outermost orbits are further from being circles. The orbits are, to a very good approximation, ellipses with an eccentricity depending on the distance to the central star for circumstellar discs, and to the centre of mass for circumbinary discs. Thus, we have calculated the m=2 Fourier mode for all the orbits given

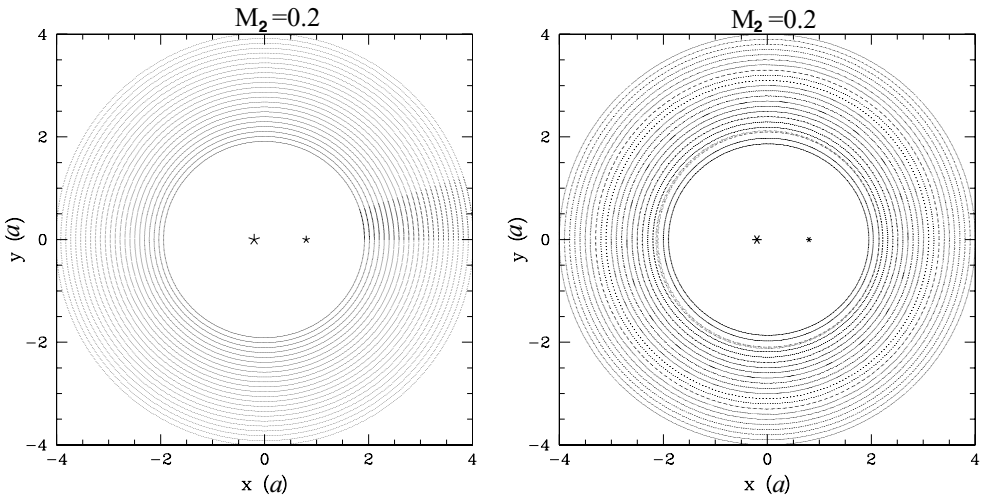

Figure 2. Comparison for a circumbinary disc between orbits obtained with the approximation presented in this work and with the numerical results described in Subsection 4.1 for the case $M_2 = 0.2$. The left panel shows the analytical approximation provided in this work, and the right panel shows the numerical approximation. The axes are in units of the distance between the stars, a. The distances of the primary and secondary stars with respect to the centre of mass of the system are indicated by the black asterisks.

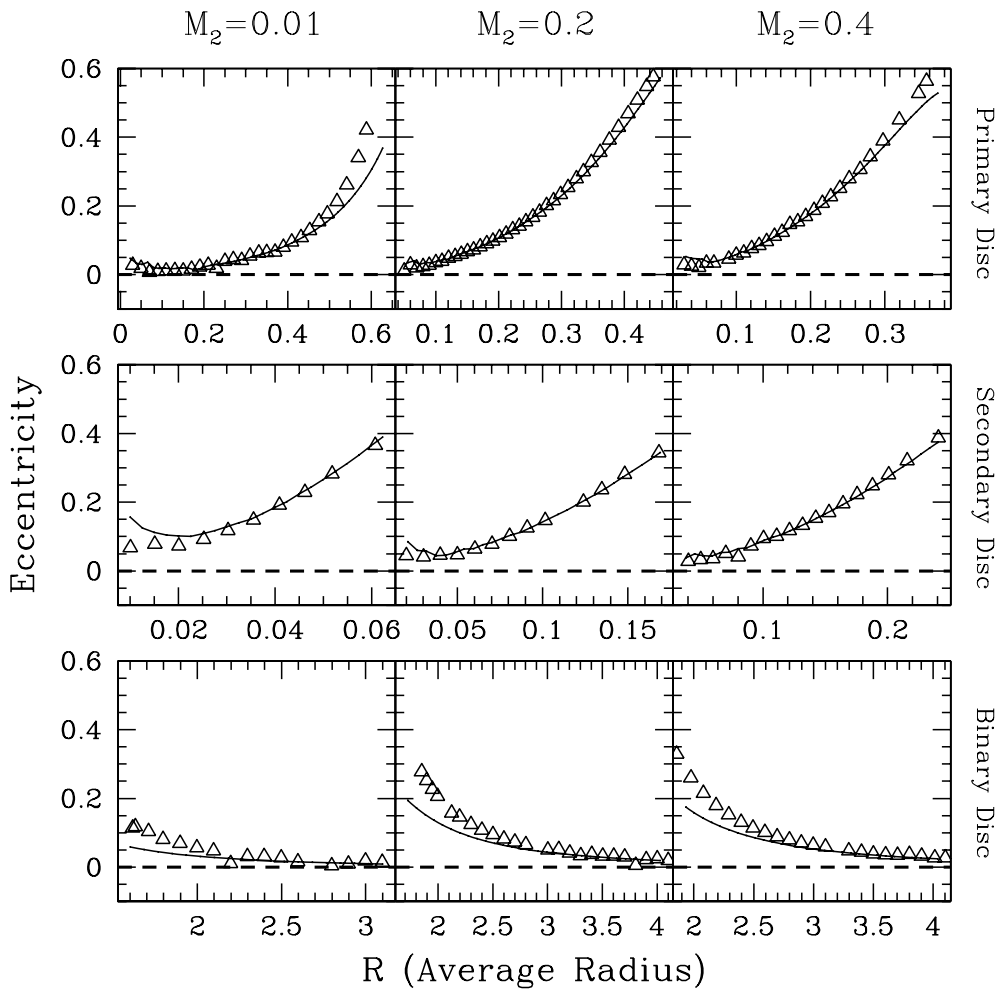

Figure 3. The orbital eccentricity versus radius produced by the analytical approximation provided in this work (continuous lines), the full numerical solution (open triangles), and, for reference, the Keplerian ($ecc = 0$) solution (dashed straight lines). The three examples of masses, $M_2 = 0.01, 0.2, 0.4$, are indicated by the upper labels for the left, middle and right panels, respectively. The upper frames refer to circumprimary discs, the middle to circumsecondary discs, and the lower to circumbinary discs.

by

$$A_k = \frac{1}{N}\sum_{i=0}^{N} s(\phi_i)cos(k\phi_i),$$
$$B_k = \frac{1}{N}\sum_{i=0}^{N} s(\phi_i)sin(k\phi_i), \tag{52}$$

where the index i refers to the number of evenly distributed (by interpolation) angle points in a given loop, N is the total number of points in the loop, and $s(\phi_i)$ is the distance to the point i from the centre of mass of the binary. In this manner, the average inner radius of a circumbinary disc is given in units of the semimajor axis a by the coefficient A_K with $k = 0$. The ellipticity (ell) is given by $\sqrt{A_k^2 + B_k^2}$ with $k = 2$ in the same units and is transformed first to the ratio b_i/a_i, where a_i, b_i are the semimajor and semiminor axes of the orbit i, and finally to the eccentricity (ecc) by

$$ecc = \sqrt{1 - ell^2}, \tag{53}$$

which represents a more sensitive geometrical characteristic of the orbits than ellipticity. We have not considered in this comparison higher Fourier modes, as they are negligible compared with the $m = 2$ mode.

In Fig. 3 we show the eccentricity versus the average radius for (i) the orbits produced by the analytical approximation provided in this work (continuous lines in the nine frames), (ii) the full numerical solution (open triangles), and (iii), for reference, the Keplerian ($ecc = 0$) solution (dashed lines). Three masses, $M_2 = 0.01, 0.2, 0.4$, in the left, middle and right panels, respectively, are shown (as indicated by the labels on the upper frames). The upper frames refer to the circumprimary discs, the middle to circumsecondary discs, and the lower to

circumbinary discs. The system of reference for each case is on the respective star for the circumstellar discs, and at the centre of origin for the circumbinary discs.

4.3 Rotation curves

We also show here, for a quantitative comparison involving positions and velocities, the rotation curves for binary systems with $M_2 = 0.01$, 0.2, 0.4.

We have constructed the rotation curves by direct differentiation of equations (6) and (7) (or more precisely of equations 50 and 51), to obtain the total velocity (v_c) in two different regions of the discs. For the primary discs we compared the rotation curves obtained along the x-axis, in the left part of the discs (where the radial velocities are negative and prograde with the rotation of the binary). For the secondary we chose to compare the rotation curves along the x-axis but in the right part of the discs (where the radial velocities are positive and prograde with the rotation of the binary). Once the velocities had been calculated, we transformed the results to the inertial frame (in the circumstellar discs) by simply adding (or subtracting, depending on the given disc) the velocity of the corresponding star, and adding or subtracting a factor $\Omega\, r$, where Ω is the angular velocity of the star and r is the radius of a given point on the rotation curve. The last step is required because of the chosen reference system in which this work solves the equations, which anchors the discs to rotate with the system.

In Figs 4 and 5 we show the outer (top panels) and inner (bottom panels) regions of the primary and secondary rotation-curve discs, respectively. In a reference system located in the primary (or in the secondary) star, measuring the angle from the line that joins the stars, the inner region corresponds to angle zero from this line, and the outer regions correspond to an angle of 180°. For both figures we plot the three cases $M_2 = 0.01$, 0.2, 0.4. The three types of lines indicate (i) the Keplerian rotation curve (filled circles); (ii) the analytical approximation

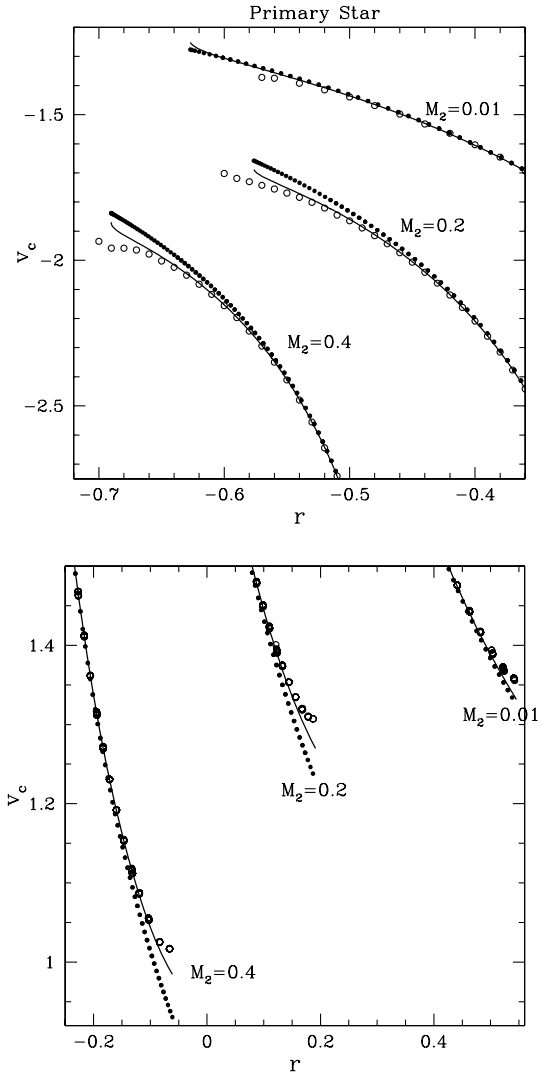

Figure 4. Comparison between the Keplerian rotation curve (filled circles), the analytical approximation provided in this work (continuous line), and the numerical solution (open circles), for the outer region (top frame) and inner region (bottom frame) of the primary disc, for $M_2 = 0.01$, 0.2, 0.4.

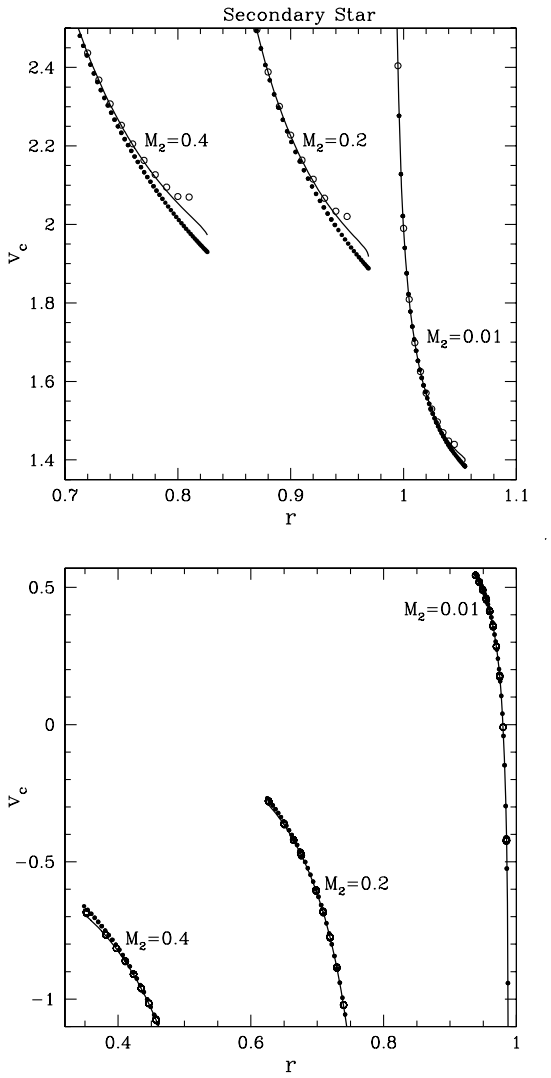

Figure 5. As Fig. 4, but for the secondary star.

provided in this work (continuous line); (iii) the numerical solution (open circles). The velocity and radius are given in code units (in such a way that $G = 1$, $M_1 + M_2 = 1$, $a = 1$ and $\Omega = 1$).

The rotation curves are in Keplerian approximately 70 per cent of the total radius of the corresponding disc. For the last 30 per cent, the Keplerian disc velocities are systematically over the numerical result, which solves the restricted three-body problem with high precision. The analytical solution we provide here is very close to the numerical solution, as expected.

In Fig. 6 we show the rotation curves as in Figs 4 and 5, but for the circumbinary disc. Although in this case both approximations (the one given in this work, and the numerical one) are very close to a Keplerian rotation curve, they are not exactly Keplerian. The velocities in the analytical approximation are systematically under the Keplerian curve and are practically the same as the ones provided by the numerical solution until near the end (the beginning of the gap), where the numerical solution goes slightly above the analytical solution. We present results for only one mass ratio, because other mass ratios would give very similar results.

In the case of the full (numerical) solution, it is worthwhile to note that we obtain in some cases discontinuities on the rotation curves and orbits, mainly as a result of resonances. This is the case, for instance, in Fig. 6, where a discontinuity very close to the resonance 3:1 ($r \sim -2.1\,a$ in the figure) is apparent. The discontinuity is also noticeable in Fig. 2 at the same radius. Owing to the perturbative fit performed in this work, finding the kind of discontinuity caused by resonances, which are in general very narrow in radius but with physics that it is highly non-linear, is outwith the scope of our approach.

5 CONCLUSIONS

We have constructed an analytical set of equations based on perturbative analysis that results in a simple and precise approximation to the solution for the circular restricted three-body problem. We chose terms in the expanded equations of motion that are relevant to the solution of the problem. The original equations were approximated with a set of equations that, in many cases, have an analytical solution. We

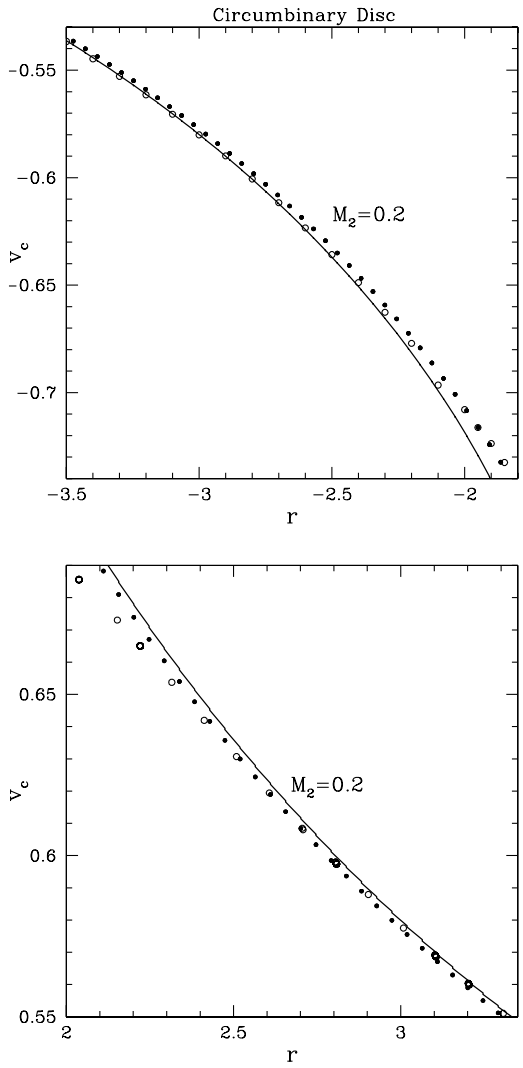

Figure 6. Comparison between the Keplerian rotation curve (filled circles), the analytical approximation provided in this work (continuous line), and the numerical solution (open circles), for the left region (top panel) and the right region (bottom panel) of the circumbinary disc, for $M_2 = 0.2$.

demonstrated the accuracy of our analytical approximation by direct comparison of geometry and rotation curves with the full numerical solution.

The set of equations we present can provide any periodic orbit for a binary system, either circumstellar or circumbinary, not only the outer-edge radius of circumstellar discs or the inner-edge radius (gap) of circumbinary discs, without the need to solve the problem numerically.

The relations provided are simple and straightforward, such that our approximation can be used for any application where initial conditions of periodic orbits or complete periodic orbits are needed, or for the direct study of the three-body restricted circular problem. For instance, in situations where it is wanted to introduce a hydrodynamical or particle code, our initial conditions would result in much more stable discs than with Keplerian initial conditions, or than would be obtained by constructing the discs directly from hydrodynamical simulations of accretion to binaries, which require long times to obtain stable discs. Because our approximation is completely analytical it will have the obvious additional advantage of being computationally extremely cheap, and easier to implement than the numerical solution.

The periodic orbits respond uniquely to the binary potential and do not consider other physical factors such as gas pressure or viscosity that are responsible for the fine details of disc structure. They are, however, the backbone of any potential, and their shape and behaviour give the general disc phase-space structure. Thus, in addition to all the possible hydrodynamical and particle disc applications, we can use them to study general disc geometry and rotation curves, or rarification and compression zones caused by orbital crowding.

ACKNOWLEDGMENTS

We thank Linda Sparke, Antonio Peimbert and Jorge Cantó for enlightening discussions. BP acknowledges project CONACyT, Mexico, through grant 50720.

REFERENCES

Bate M. R., 1997, MNRAS, 285, 16
Bate M. R., Bonnell I. A., 1997, MNRAS, 285, 33
Bonnell I., Bastien P., 1992, in McAlister H. A., Hartkopf W. I., eds, ASP Conf. Ser. Vol. 135, Complementary Approaches to Double and Multiple Star Research. Kluwer, Dordrecht, p. 206
Butler R. P., Marcy G. W., Williams E., Hauser H., Shirts P., 1997, ApJ, 474, 115
Cochran W. D., Hatzes A. P., Butler R. P., Marcy G. W., 1997, ApJ, 483, 457
Duquennoy A., Mayor M., 1991, A&A, 248, 485
Eggleton P. P., 1983, ApJ, 268, 368
Fischer D. A., Marcy G. W., 1992, ApJ, 396, 178
Holman M. J., Wiegert P. A., 1999, AJ, 117, 621
Lubow S. H., Shu F. H., 1975, ApJ, 198, 383
Mathieu R. D., 1994, ARA&A, 32, 465
Mathieu R. D., Ghez A. M., Jensen E. L. N., Simon M., 2000, in Mannings V., Boss A. P., Russell S. S., eds, Protostar and Planets IV. Univ. Arizona Press, Tucson, p. 731
Message P. J., 1959, AJ, 64, 226
Moulton F. R., 1963, Periodic Orbits. Carnegie Institution of Washington, Washington, p. 1920
Murray C. D., Dermott S. F., 1999, Solar System Dynamics. Cambridge Univ. Press, Cambridge, p. 229
Paczyński B., 1977, ApJ, 216, 822 (PSA05)
Papaloizou J., Pringle J. E., 1977, MNRAS, 181, 441
Pichardo B., Sparke L. S., Aguilar L. A., 2005, MNRAS, 359, 521
Rodríguez L. F. et al., 1998, Nat, 395, 355
Rudak B., Paczyński B., 1981, Acta Astron., 31, 13
Wiegert P. A., Holman M. J., 1997, AJ, 113, 1445

This paper has been typeset from a TEX/LATEX file prepared by the author.